The Differential Effects of Mutant *p53* Alleles on Advanced Murine Lung Cancer

Erica L. Jackson,[1] Kenneth P. Olive,[1] David A. Tuveson,[2] Roderick Bronson,[3] Denise Crowley,[1] Michael Brown,[1] and Tyler Jacks[1,4]

[1]Center for Cancer Research, Massachusetts Institute of Technology, Cambridge, Massachusetts; [2]Abramson Family Cancer Research Institute, University of Pennsylvania, Philadelphia, Pennsylvania; [3]Department of Pathology, Tufts University School of Medicine and Veterinary Medicine, Boston, Massachusetts; and [4]Howard Hughes Medical Institute, Chevy Chase, Maryland

Abstract

We report a direct comparison of the differential effects of individual p53 mutations on lung tumor growth and progression, and the creation of a murine model of spontaneous advanced lung adenocarcinoma that closely recapitulates several aspects of advanced human pulmonary adenocarcinoma. We generated compound conditional knock-in mice with mutations in *K-ras* combined with one of three *p53* alleles: a contact mutant, a structural mutant, or a null allele. *p53* loss strongly promoted the progression of *K-ras*–induced lung adenocarcinomas, yielding a mouse model that is strikingly reminiscent of advanced human lung adenocarcinoma. The influence of *p53* loss on malignant progression was observed as early as 6 weeks after tumor initiation. Furthermore, we found that the contact mutant $p53^{R270H}$, but not the structural mutant $p53^{R172H}$, acted in a partially dominant-negative fashion to promote *K-ras*–initiated lung adenocarcinomas. However, for both mutants, loss-of-heterozygosity occurred uniformly in advanced tumors, highlighting a residual tumor-suppressive function conferred by the remaining wild-type allele of p53. Finally, a subset of mice also developed sinonasal adenocarcinomas. In contrast to the lung tumors, expression of the point-mutant *p53* alleles strongly promoted the development of sinonasal adenocarcinomas compared with simple loss-of-function, suggesting a tissue-specific gain-of-function. (Cancer Res 2005; 65(22): 10280-8)

Introduction

Lung cancer is the leading cause of cancer deaths worldwide, with 157,200 deaths predicted for the year 2003 in the United States alone (1). Adenocarcinoma, a subtype of non–small-cell lung cancer, is the single most common form of lung cancer, comprising ~40% of cases (1). Activating mutations in the *K-ras* proto-oncogene are found in ~30% of human non–small-cell lung cancers (2). Recently, several mouse lung cancer models have been created using conditionally or spontaneously activatable alleles of oncogenic *K-ras* (3–6). These models have contributed significantly to our understanding of the role of *K-ras* in tumor initiation and maintenance of the tumor phenotype but do not recapitulate all aspects of the human disease. In particular, the lung tumors in these models resemble early-stage human lung adenocarcinoma. Features of late-stage disease including invasion, stromal desmoplasia, and metastasis are not prominent.

Alterations in the *p53* tumor suppressor gene are also common in non–small-cell lung cancer, occurring in ~50% of cases (7). As in other cancers, the majority of these alterations are missense mutations that result in the accumulation of high levels of mutant p53 protein. Missense mutations in *p53* occur primarily in the DNA-binding domain but the frequency of mutation at individual codons varies dramatically between tumor types. The most common *p53* missense mutations in human pulmonary adenocarcinomas occur in descending order at codons 273, 248, 249, 245, and 158 (8). Of note, codon 175 mutations are significantly less common in lung adenocarcinomas than in other cancers. This discrepancy is typically explained by the fact that different codons vary in their exposure and susceptibility to mutagens. About 90% of lung tumors are associated with exposure to carcinogens from tobacco smoke and the polycyclic aromatic hydrocarbons found in tobacco smoke preferentially bind to and form adducts with several of the p53 codons frequently mutated in lung cancer. However, these compounds also efficiently form adducts at codon 175, weakening this theory (9).

An alternative explanation for the variation in mutation frequency between tumor types is a difference in the tumorigenic potential of individual mutant p53 proteins in different tissues. *p53* mutations are commonly grouped into two classes that display different behaviors in several *in vitro* assays (10). Contact mutations alter residues that directly contact DNA whereas structural mutations alter residues that are critical for maintaining global domain structure (11). Structural mutants are frequently described as more potent than contact mutants in promoting cancer. In general, point-mutant *p53* confers an adverse prognosis in patients with pulmonary adenocarcinoma but the tumorigenicity of individual mutations has not been determined (12, 13).

Tumor-derived *p53* mutations may have two effects beyond loss of function. There is evidence that mutant *p53* alleles can act in a dominant-negative manner to inhibit the function of wild-type *p53* through hetero-oligomerization between mutant and wild-type p53 polypeptides. *In vitro* studies have shown that both classes of mutants can exert dominant-negative effects on wild-type p53 activity with the effects being stronger for structural mutants (14). Furthermore, certain point-mutant *p53* alleles have been shown to promote tumorigenesis through gain-of-function effects that are not dependent on wild-type *p53* (15).

We recently generated two strains of conditional point-mutant p53 mice that allow for endogenous expression of mutant p53 on Cre-mediated recombination. The first strain carries the contact mutation $p53^{R270H}$ (homologous to human $p53^{R273H}$) whereas the second strain carries the structural mutation $p53^{R172H}$ (homologous to human $p53^{R175H}$; ref. 16).

Note: E.L. Jackson and K.P. Olive contributed equally to this work. T. Jacks is an Investigator of Howard Hughes Medical Institute. K.P. Olive is a David Koch fellow.

Requests for reprints: Tyler Jacks, Center for Cancer Research, Massachusetts Institute of Technology, Building E17-517A, 77 Massachusetts Avenue, Cambridge, MA 02141. Phone: 617-253-0263; Fax: 617-253-9863; E-mail: tjacks@mit.edu.

©2005 American Association for Cancer Research.

doi:10.1158/0008-5472.CAN-05-2193

Downloaded from http://aacrjournals.org/cancerres/article-pdf/65/22/10280/2538761/10280-10288.pdf by guest on 27 March 2025

We report here the creation of an improved murine lung cancer model through the generation of compound mutant animals with conditional mutations in *K-ras* and *p53*. This model closely recapitulates several aspects of advanced human pulmonary adenocarcinoma not commonly seen in existing models. We have used this model to directly compare the oncogenic properties of different *p53* mutations ($p53^{R270H}$, $p53^{R172H}$, and a large deletion mutation of p53) in the context of a single tumor type initiated by a defined oncogenic stimulus. Our comparison of *K-ras*-induced lung tumors with mutant or null alleles of p53 clearly shows a dominant-negative effect by the $p53^{R270H}$ allele that is not conferred by the $p53^{R172H}$ allele. Furthermore, we describe a tissue-specific gain of oncogenic potential conferred by both the $p53^{R172H}$ and the $p53^{R270H}$ alleles toward the development of carcinomas of the sinonasal mucosa.

Materials and Methods

Breeding schemes. *LSL-K-ras*^{G12D} mice were crossed to $p53^{Fl/+}$ mice to generate *LSL.K-ras*^{G12D};$p53^{Fl/+}$ (K;Fl/+) mice. The $p53^{R172H}$ and $p53^{R270H}$ strains were each crossed to the $p53^{Fl}$ strain to generate $p53^{R172H/Fl}$ and $p53^{R270H/Fl}$ mice. By crossing K;Fl/+ mice with $p53^{R172H/Fl}$ and $p53^{R270H/Fl}$ mice, offspring of the following genotypes were generated for use in tumor studies: K;Fl/+, K;172/+, K;Fl/Fl, K;172/Fl, K;270/+, and K;270/Fl.

Molecular analysis of recombination efficiency. DNA was prepared from dissected tumors. For the *K-ras* allele, PCR was done using the Advantage-GC-cDNA kit from Clontech (Mountain View, CA) with primers flanking the lox-stop-lox cassette: K5′-1 forward, 5′-GGGTAGGTGTTGGGA-TAGCTG-3′, and K3′-3 reverse, 5′-TCCGAATTCAGTGACTACAGATGTACA-GAG-3′. The wild-type and recombined conditional *K-ras* alleles yield 265- and 305-bp products, respectively. Analysis of the conditional *p53* point-mutant alleles was done using standard PCR buffer with primers flanking the lox-stop-lox cassette: dt020200.1 forward, 5′-AGCCTGCCTAGCTTCCT-CAGG-3′, and dt011200.3 reverse, 5′-CTTGGAGACATAGCCACACTG-3′. The wild-type and Flox *p53* alleles produce a 291-bp product and the recombined conditional allele produces a 325-bp product. PCR analysis of the floxed allele was done using standard PCR buffer with primers flanking the loxP sites in exons 2 and 10: forward, 5′-CACAAAAACAGGTTAACCCAG-3′, and reverse, 5′-GAAGACAGAAAAGGGGAGGG-3′. The recombined allele yields a 612-bp product; no product is produced from the wild-type allele.

AdenoCre infection. Mice were infected with 5×10^5 plaque-forming units (pfu) of AdenoCre virus at 6 to 8 weeks of age. AdenoCrE:CaPi coprecipitates were prepared as described (17). Mice were anesthetized with avertin. AdenoCre:CaPi coprecipitates were administered intranasally in two 62.5-μL instillations.

Tissue harvesting. Mice were sacrificed by CO_2 asphyxiation. The trachea was exposed and the lungs were inflated with formalin. All tissues were fixed in formalin overnight at room temperature and then placed into 70% ethanol and sent for processing through paraffin. Once processed, each lobe of the lung was cut in a set pattern and embedded in paraffin. Remaining organs were embedded according to standard protocols.

Immunohistochemistry and trichrome staining. All lungs were sectioned as follows: five-step sections were taken at 100 μm apart, with five unstained sections taken after section 3. p53 immunohistochemistry was done following Trilogy dewaxing/unmasking according to instructions of the manufacturer. *p53* CM5 rabbit polyclonal antibody (Novo Castra, Newcastle upon Tyne, United Kingdom) was used at a 1:500 dilution. Staining was completed with a horseradish peroxidase anti-rabbit kit (Vector Labs). For phospho-mitogen-activated protein kinase (MAPK) immunohistochemistry, high-temperature citrate buffer unmasking was done and anti–phospho-p42/44MAPK (Cell Signaling, Beverly, MA) was diluted 1:100. Sections were incubated in primary antibody overnight at 4°C. Trichrome staining was done using a Masson's trichrome kit from Poly Scientific R&D (Bayshore, NY).

Tumor grading. Tumor grading was done without knowledge of genotype on the level 3 section of each lung. Each tumor was given a score of 1 to 5 based on predetermined criteria (see Results for specific grading criteria).

Tumor size measurement. Lung and tumor areas were determined using Bioquant Image Analysis software in manual measurement mode.

Results

Generation of K-ras/p53 compound conditional mutant mice. To assess the effect of *p53* mutation or loss on *K-ras*-induced lung tumorigenesis, compound mutant mice were generated that harbored the conditional activatable *LSL-K-ras*^{G12D} allele (6, 18) and combinations of three different conditional *p53* alleles: $p53^{LSL.R270H}$, $p53^{LSL.R172H}$, and $p53^{Flox}$ (refs. 16, 19; Fig. 1*A*). For clarity, the genotypes of the compound mutant mice will be described in this article using the following abbreviations; the conditional *LSL-K-ras*^{G12D} allele will be referred to as K and the wild-type *p53*, $p53^{LSL.R270H}$, $p53^{LSL.R172H}$, and $p53^{Flox}$ alleles will be referred to as +, 270, 172, and Fl, respectively. The compound mutant mice will be referred to collectively as K,P mice. The following K,P mice were generated: K;Fl/+, K;270/+, K;172/+, K;Fl/Fl,

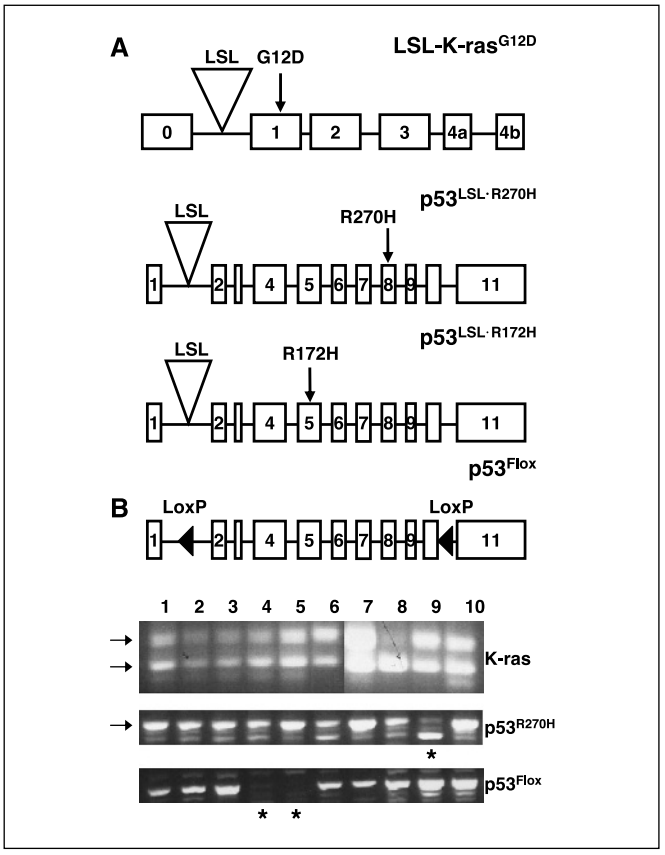

Figure 1. Generation of K,P compound mutant mice. *A,* diagram of *K*-ras and *p53* conditional alleles. The *LSL-K-ras*^{G12D} allele contains an activating mutation at codon 12 and a Lox-Stop-Lox (*LSL*) cassette inserted into intron 0 upstream of the transcriptional start site. The $p53^{LSL.R172H}$ and $p53^{LSL.R270H}$ alleles contain an Arg→His mutation in exons 5 and 8, respectively, and a LSL cassette in intron 1. The $p53^{Flox}$ allele encodes the wild-type p53 protein and contains LoxP sites flanking exons 2 and 10. *B,* recombination efficiency of conditional alleles. Genomic DNA was isolated from 10 different K;270/Fl tumors (*lanes 1-10*). *Top,* to assess recombination of the *LSL-K-ras*^{G12D} allele, PCR was done using primers flanking the LSL cassette. The recombined *K-ras*^{G12D} and wild-type alleles yield 305-bp (*top arrow*) and 265-bp (*bottom arrow*) products, respectively. *Middle,* PCR analysis of the p53 locus using primers flanking the LSL cassette in intron 1. The 335-bp product (*arrow*) is produced from the recombined conditional allele. *Asterisk,* unrecombined sample. *Bottom,* PCR analysis of the $p53^{Fl}$ allele using primers flanking exons 2 and 10. The recombined $p53^{Fl}$ allele produces a 612-bp product. No product is produced from the unrecombined allele (*asterisks*).

Downloaded from http://aacrjournals.org/cancerres/article-pdf/65/22/10280/2538761/10280-10288.pdf by guest on 27 March 2025

K;270/Fl, and K;172/Fl, allowing us to examine the effects of point-mutant p53 proteins in the presence and absence of wild-type p53 compared with the complete loss of p53. Crosses were designed to minimize effects of mixed genetic backgrounds (see Materials and Methods). Cohorts of K,P mice were infected with 5×10^5 pfu of a recombinant adenovirus expressing Cre recombinase (AdenoCre) by intranasal instillation and then sacrificed at various time points (described below). As expected, all of the mice developed multiple primary lung tumors following infection with AdenoCre.

Infection with AdenoCre induces recombination of the conditional alleles. To assess the recombination efficiency of each allele when multiple alleles were present, DNA was isolated from tumors dissected from the lungs of K;270/Fl mice and PCR was done to detect recombination. The $p53^{R270H}$ and the $p53^{R172H}$ alleles only differ at the single base mutations downstream of the LSL cassette, so the recombination of these alleles was assumed to be identical. In every tumor, PCR amplification of the *K-ras* allele produced a product 40 bp larger than the wild-type allele due to the single loxP site remaining after Cre-mediated recombination (Fig. 1*B, top*). Therefore, the $K\text{-}ras^{G12D}$ allele recombined with 100% efficiency. Similar analyses showed that the $p53^{LSL.R270H}$ allele recombined in 90% (9 of 10) of the tumors analyzed (Fig. 1*B, middle*). The recombination efficiency of the $p53^{Flox}$ allele was comparable, occurring in 80% (8 of 10) of tumors analyzed (Fig. 1*B, bottom*).

Loss of p53 function promotes malignant progression of lung tumors. To investigate the effects of p53 loss, we evaluated the lung tumor phenotypes of K;Fl/+ and K;Fl/Fl mice at various time points after AdenoCre infection. A cohort of K;Fl/+ mice were euthanized at a late time point (26 weeks) after infection. The tumors present in K;Fl/+ mice resembled those seen previously in $L\text{-}K\text{-}ras^{G12D}$ single mutant mice, ranging from adenomas to early-stage adenocarcinomas (6). This indicates that the loss of a single copy of p53 does not significantly affect the progression of K-ras-initiated lung adenocarcinomas.

A cohort of K;Fl/Fl mice was also generated for analysis at this time point. However, it became apparent that these mice would not survive for 26 weeks after infection, so they were sacrificed after 19 weeks. In contrast to the K;Fl/+ mice, all of the K;Fl/Fl animals had advanced pulmonary adenocarcinomas. Multiple tumors were present in each mouse ranging from well-differentiated tumors to advanced highly dysplastic lesions containing large sheets of dysplastic cells, abnormal mitoses, and multinucleate giant cells.

To quantify the extent of progression of K;Fl/Fl tumors, we devised a grading system by which to evaluate the stage of every tumor in each mouse. Tumors were scored in a blinded manner on a scale of 1 to 5 with grade 5 indicating the most advanced tumor phenotype. The criteria for each grade are as follows: Grade 1 tumors have uniform nuclei showing no nuclear atypia. Grade 2 tumors contain cells with uniform but slightly enlarged nuclei that exhibit prominent nucleoli. Grade 3 tumors have cells with enlarged, pleomorphic nuclei showing prominent nucleoli and nuclear molding. Grade 4 tumor cells have very large, pleomorphic nuclei exhibiting a high degree of nuclear atypia, including abnormal mitoses and hyperchromatism, and contain multinucleate giant cells. Grade 5 tumors have all the features of grade 4 tumors and also show stromal desmoplasia surrounding nests of tumor cells (see Fig. 2 for examples).

Using this grading scheme to analyze 944 tumors from 12 K;Fl/+ mice and 1161 tumors from 15 K;Fl/Fl mice, we confirmed that loss of p53 resulted in a markedly more severe tumor phenotype in K-ras-initiated lung adenocarcinomas (Fig. 3*A*). In addition, K;Fl/Fl tumors showed several characteristics of human lung tumors that were lacking in previous murine lung cancer models (20). Perhaps, most striking was the presence of tumors containing a large stromal component in which nests of tumor cells could be found growing within a field of desmoplastic stroma (Fig. 3*B*). Masson's trichrome staining of these tumors showed the abundant production of collagen by the stromal fibroblasts (Fig. 3*C*) and immunohistochemistry confirmed the expression of smooth muscle actin by some of the stromal fibroblasts (data not shown).

A subset of K;Fl/Fl tumors was highly invasive, growing into the hilus, heart, and overlying pleura (Fig. 3*D*). Furthermore, tumor cells were observed along the luminal surfaces of blood and lymphatic vessels within the tumor mass (data not shown) showing extravasation of the tumor cells, which is required for metastatic spread. In addition, lymph node metastases were present in over 50% (8 of 15) of K;Fl/Fl mice (Fig. 3*E*) and a small percentage had metastases to distant organs (Fig. 3*F*).

Having established that *p53* loss accelerates the progression of K-ras-initiated lung adenocarcinomas, we were curious how rapidly this contributed to tumor progression. Therefore, we examined the lungs of K;Fl/+ and K;Fl/Fl mice 6 weeks after infection with AdenoCre. The lungs of K;Fl/+ mice contained lesions ranging from atypical adenomatous hyperplasia to small adenomas (Fig. 4*A*). The adenomas present in these mice were very small and, with rare exceptions, had regular nuclei (Fig. 4*B*). Atypical adenomatous hyperplasia and adenomas were also present in K;Fl/Fl mice but were often larger and frequently displayed nuclear atypia (Fig. 4*C*). Even some of the smallest lesions had aberrant nuclei (Fig. 4*D*) and a few tumors even contained multinucleate giant cells (Fig. 4*C*). Grading of 111 tumors from 12 K;Fl/+ mice and 215 tumors from K;Fl/Fl mice showed a clear shift ($P < 0.001$) towards more malignant lesions in K;Fl/Fl mice (Fig. 4*A*), indicating that p53 loss promotes rapid lung tumor progression.

A partial dominant-negative effect by the $p53^{R270H}$ allele towards malignant progression. Endogenous expression of mutant *p53* can result in a gain-of-function effect on tumor development in some tissues (16, 21). Therefore, we examined whether endogenous expression of point-mutant *p53* in K-ras-initiated lung adenocarcinomas would result in a more severe tumor phenotype than homozygous deletion of *p53*. Cohorts of K;270/Fl and K;172/Fl mice were sacrificed 19 weeks after AdenoCre infection and their lung tumors were compared with K;Fl/Fl mice described above. Surprisingly, grading of 841 tumors from 11 K;270/Fl mice and 839 tumors from 10 K;172/Fl mice did not reveal any differences in the distribution of tumor grades compared with K;Fl/Fl mice (Fig. 5*A*). All three genotypes had substantially fewer low-grade and more high-grade tumors than K;Fl/+ animals sacrificed at 26 weeks postinfection, and all had tumors that were highly invasive and often metastatic to the regional lymph nodes. Together, these data support the loss of wild-type *p53* function as a factor in the progression of K-ras-initiated lung adenocarcinomas but do not support a gain-of-function effect by point-mutant p53 in these tumors.

The absence of a gain-of-function effect allowed us to cleanly evaluate the role of dominant-negative effects of mutant p53 in the progression of K-ras-initiated lung adenocarcinomas. Cohorts of K;270/+ and K;172/+ mice were sacrificed 26 weeks after AdenoCre infection and compared with K;Fl/+ mice described above. Grading was done on 932 tumors from 11 K;270/+ mice and 773 tumors from 10 K;172/+ mice. Strikingly, whereas the distribution of tumor grades was similar between K;Fl/+ and K;172/+ mice, the K;270/+

Downloaded from http://aacrjournals.org/cancerres/article-pdf/65/22/10280/2538761/10280-10288.pdf by guest on 27 March 2025

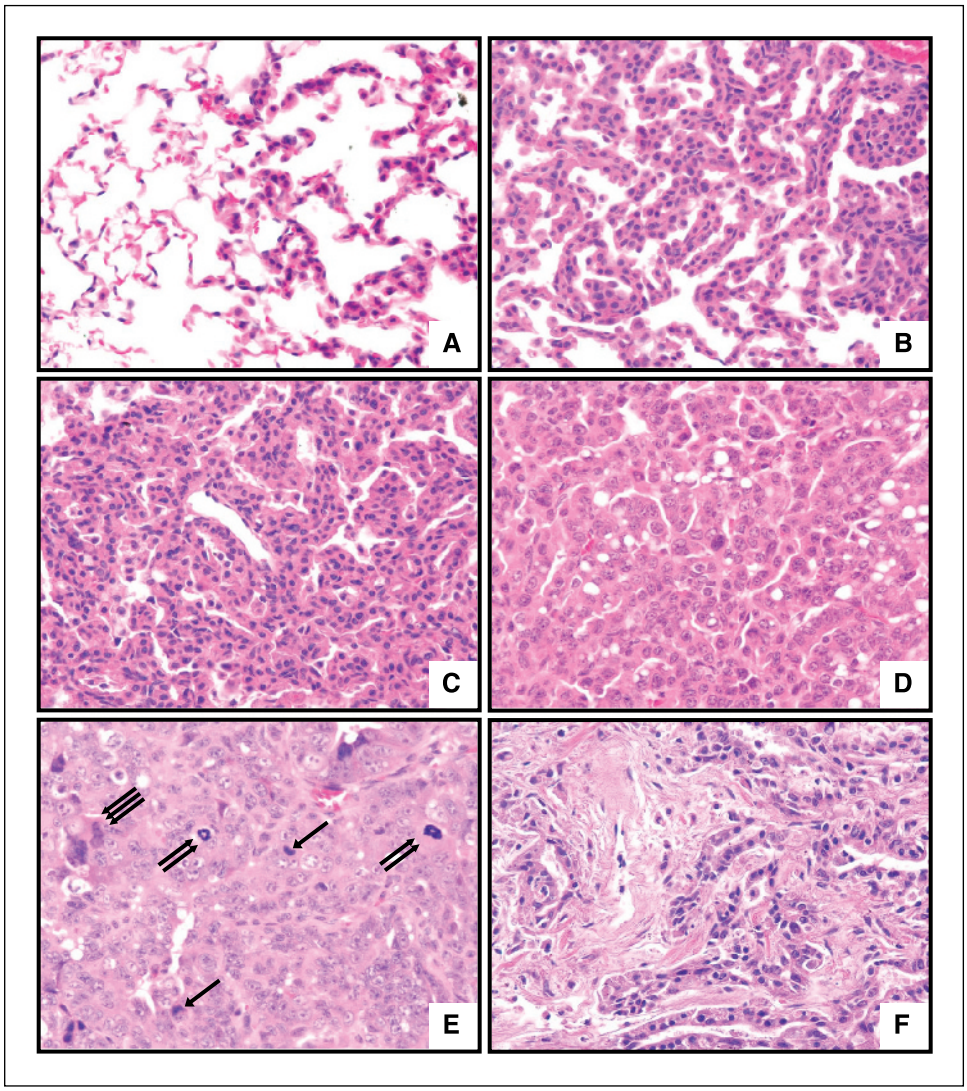

Figure 2. Tumor grades in K,P compound conditional mutant mice. *A,* a region of advanced adenomatous hyperplasia, adjacent to normal lung (*left*). Hyperplastic cells are enlarged and may accumulate slightly but generally follow the underlying lung architecture. *B,* grade 1 lesions form a solid tumor but have regular nuclei. *C,* grade 2 lesions may have slightly irregular nuclei and prominent nucleoli. *D,* cells in grade 3 lesions exhibit pleomorphic nuclei, prominent nucleoli, and nuclear molding. *E,* grade 4 lesions have enlarged, pleomorphic nuclei (*single arrows*), aberrant mitoses (*double arrows*), and tumor giant cells (*triple arrows*). *F,* grade 5 lesions exhibit all the criteria of grade 4 lesions as well as nests of tumors cells surrounded by a desmoplastic stroma.

mice displayed a significant shift in the tumor distribution (χ^2, $P < 0.001$) with fewer low-grade and more high-grade tumors (Fig. 5*A* and *B*). Therefore, $p53^{R270H}$, but not $p53^{R172H}$, acted as a partial dominant-negative allele in the development of high-grade lung adenocarcinoma.

To determine whether this effect also extended to the size of the tumors, we examined the tumor burden after 26 weeks of growth. The average number of tumors in K;Fl/+, K;172/+, and K;270/+ mice were similar (79 ± 21, 77 ± 24, and 85 ± 17, respectively). We measured tumor burden as the percentage of total lung occupied by tumor. Like the grading results, we found that K;Fl/+ and K;172/+ mice had similar tumor burdens with tumor occupying 24% and 27% of the total lung area, respectively. However, the tumor burden in K;270/+ mice was consistently higher, with tumor comprising 36% of the total lung area ($P = 0.024$; Fig. 5*C*). These findings further support a dominant-negative effect specifically conferred by the $p53^{R270H}$ allele on lung tumor growth and progression.

Up-regulation of the Raf/mitogen-activated protein kinase pathway occurs in advanced tumors. Studies in primary fibroblasts have linked high levels of Raf/MAPK activity to Ras-induced premature senescence, in part through activation of p19ARF, a positive regulator of p53 (22). Therefore, we reasoned that mutation of p53 might allow for up-regulation of this signaling pathway, which could account for its tumor-promoting effects. To address this question, immunohistochemistry was done on both early- and late-stage tumors from the K,P mice of all six genotypes using anti–phospho-p42/44MAPK antibodies.

At 6 weeks postinfection, no phospho-MAPK positive tumors were present in any of the animals evaluated, indicating that loss of p53 alone is not sufficient to allow up-regulation of the Raf/MAPK pathway. However, a subset of late-stage tumors contained large foci of phospho-MAPK positive cells and sometimes the entire tumors were immunoreactive. The percentage of phospho-MAPK positive tumors varied depending on the p53 genotype (Fig. 5*D*). Roughly half of the tumors in K;Fl/Fl, K;172/Fl, and K;270/Fl animals stained positively for phospho-MAPK (52.2%, 51.2%, and 50.6% respectively). Strikingly, the frequency of MAPK activation was identical in K;270/+ mice, occurring in 53.1% of the tumors, whereas only 13.7% of K;Fl/+ tumors were phospho-MAPK positive. Therefore, although p53 loss alone is not sufficient to enable up-regulation of the Raf/MAPK pathway, it may promote the accumulation of additional events that allow MAPK activation. Furthermore, the $p53^{R270H}$ allele dominantly interferes with the ability of wild-type p53 to restrain MAPK up-regulation.

Downloaded from http://aacrjournals.org/cancerres/article-pdf/65/22/10280/2538761/10280-10288.pdf by guest on 27 March 2025

Wild type–specific loss of heterozygosity in K;270/+ tumors despite dominant-negative effects by the $p53^{R270H}$ allele. To determine whether the dominant-negative effect of the $p53^{R270H}$ allele alleviates the selective pressure to lose the wild-type allele of p53, we examined the frequency of loss of heterozygosity (LOH). Quantitative PCR analysis was done on genomic DNA isolated from tumors microdissected from the lungs of K;Fl/+ and K;270/+ mice using TaqMan MGB probes. For both genotypes, 100% of the tumors analyzed (n = 11 for K;270/+ and n = 8 for K;Fl/+) showed loss of the wild-type *p53* allele. These data show that there is still selective pressure for full loss of p53 function despite the dominant-negative effects of the $p53^{R270H}$ allele. This may explain why the tumors found in K;270/+ mice, although larger and more advanced than those in K;Fl/+ mice, were not as large and advanced as those in K;Fl/Fl mice, and may help to explain the wild type–specific p53 LOH that is frequently observed in human tumors (12, 13, 23).

Mutant p53 promotes the development of sinonasal adenocarcinomas. The method of AdenoCre administration used here exposes the entire respiratory tract to the virus. Thus, infection and subsequent recombination of the conditional alleles could occur in cells of the nasal passages or the trachea. However, none of the conditional $K\text{-}ras^{G12D}$ single mutant mice developed tumors in the upper respiratory tract, suggesting that the expression of $K\text{-}ras^{G12D}$ in these cells is not sufficient to induce tumorigenesis. In the course of performing the experiments described above, we observed that K;172/Fl and K;270/Fl compound mutant mice had a higher mortality than K;Fl/Fl compound mutants, which could not be explained by differences in their lung tumor phenotype, as there was none. Histologic analysis of head sections revealed the presence of anaplastic adenocarcinomas in the nasal passages of a subset of the 19-week K;Fl/Fl, K;270/Fl, and K;172/Fl mice that seemed to arise from the mucous glands of the nasal sinuses. The tumors were extremely poorly differentiated but pan-cytokeratin immunostaining confirmed their epithelial origin (data not shown). The tumor cells displayed dramatically pleomorphic, vesiculated nuclei with prominent nucleoli (Fig. 6*B*). Furthermore, the tumors were destructively invasive, often penetrating through the cribriform plate into the olfactory bulb (Fig. 6*C*).

Consistent with their increased mortality, the incidence of sinonasal adenocarcinomas was >4-fold higher in K;172/Fl (64%) and K;270/Fl (69%) mice than in p53Fl/Fl (14%) mice (Fig. 6*D*). The increased incidence of tumors in K;270/Fl and K;172/Fl mice was

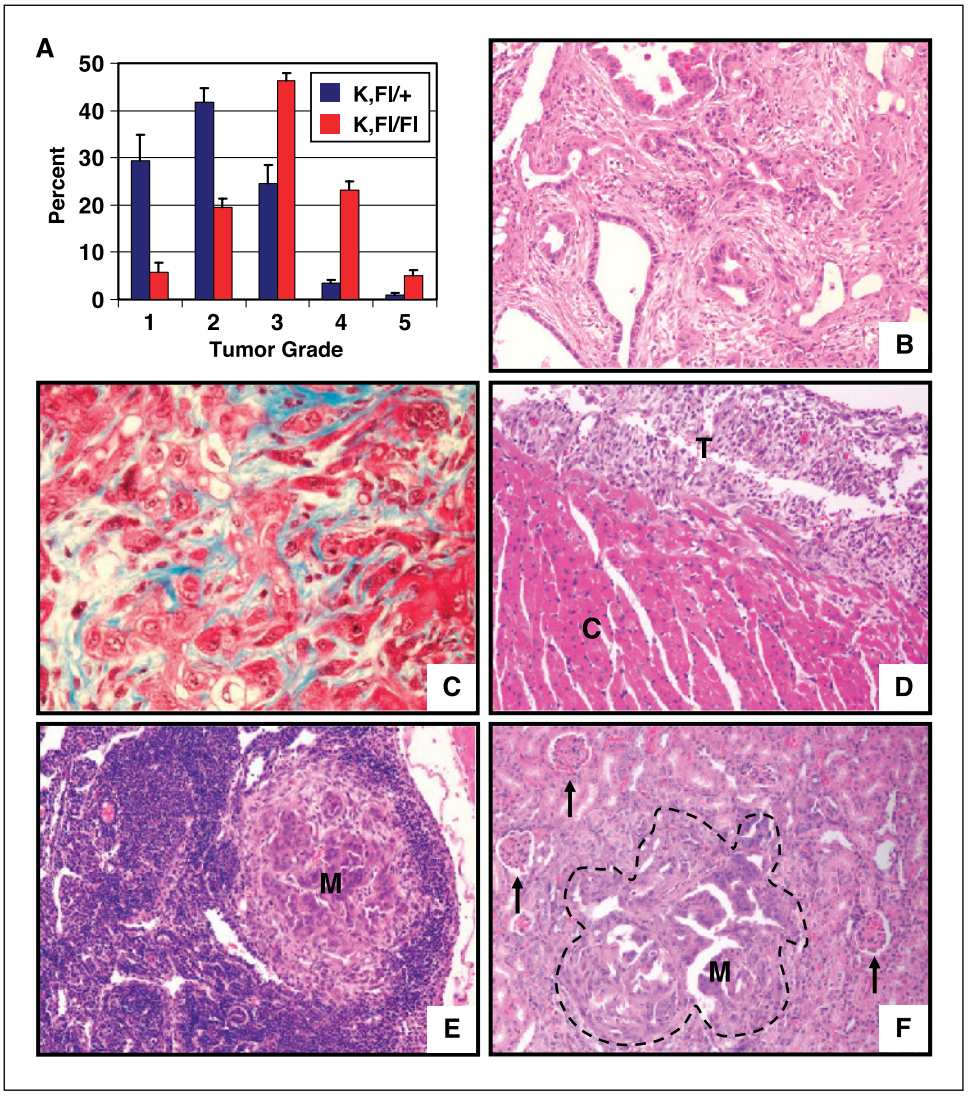

Figure 3. Loss of *p53* results in progression of *K-ras*-induced lung adenocarcinomas. Slides are stained with H&E unless otherwise indicated. *A,* distribution of tumor grades in K;Fl/+ mice (*blue columns*) and K;Fl/Fl mice (*red columns*). *Columns,* percent of total tumors for each grad; *bars,* SE. *B,* a region of stromal desmoplasia with invasion of tumor cells in a grade 5 tumor; ×200. *C,* Masson's trichrome stained section of a tumor with tumors cells (*red*) invading a region of collagen-containing stroma (*blue*); ×400. *D,* section of a lung adenocarcinoma (*T*) invading adjacent cardiac muscle (*C*); ×200. *E,* section of a lung adenocarcinoma metastasis (*M*) in a thoracic lymph node; ×100. *F,* section of a distal lung tumor metastasis (*M*) to the kidney. *Arrows,* normal glomeruli in the kidney; *dashed line,* boundary of the metastasis.

Downloaded from http://aacrjournals.org/cancerres/article-pdf/65/22/10280/2538761/10280-10288.pdf by guest on 27 March 2025

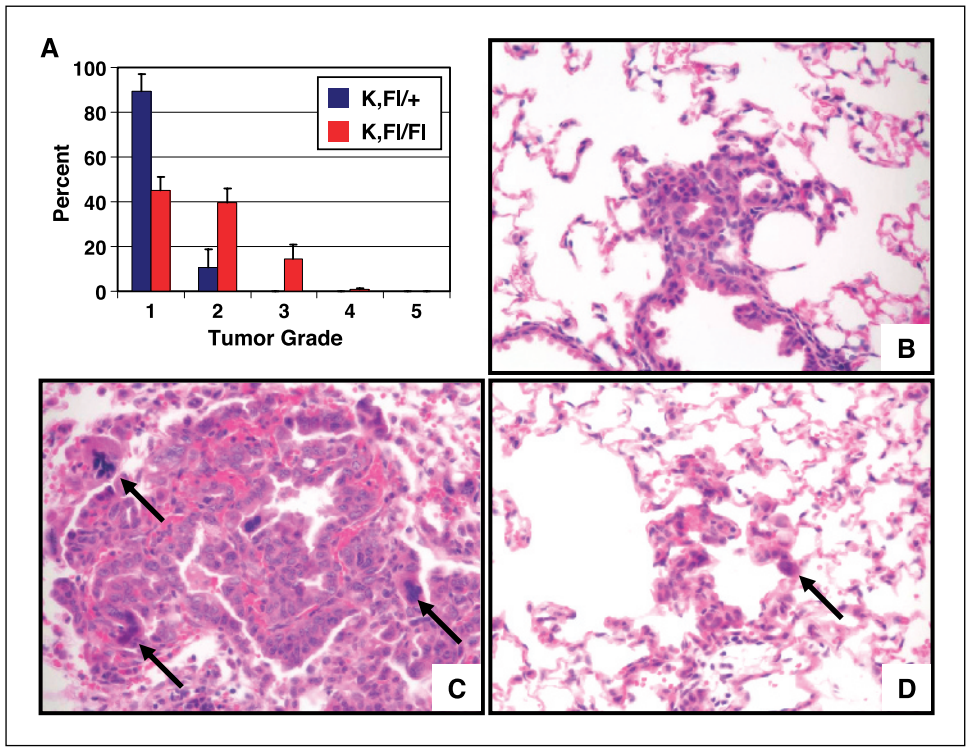

Figure 4. Effects of *p53* loss are apparent six weeks after AdenoCre infection. Slides are stained with H&E. *A,* distribution of tumor grades in K;Fl/+ (*blue columns*) and K;Fl/Fl mice (*red columns*). *Columns,* percent of total tumors for each grade; *bars,* SE. *B,* section of a lesion from a K;Fl/+ mouse, 6 weeks postinfection with AdenoCre. Nuclei are regular and retain apical/basal polarity; ×400. *C,* section of a lesion from a K;Fl/Fl mouse, 6 weeks postinfection with 5×10^5 pfu of AdenoCre. *Arrows,* several enlarged cells with aberrant nuclei; ×400. *D,* an example of a very small lesion from a K;Fl/Fl mouse, 6 weeks postinfection with 5×10^5 pfu of AdenoCre. Tumor cells have irregular nuclei, including one enlarged, aberrant cell (*arrow*); ×400.

highly statistically significant (χ^2, $P = 0.001$). Given the significantly higher incidence of sinonasal carcinoma on expression of point-mutant p53 compared with loss of p53 expression, these data provide strong evidence for a gain of oncogenic potential by point-mutant p53 *in vivo*.

Discussion

In this work, we present compound mutant mice incorporating somatically manipulatable conditional mutations in the *K-ras* proto-oncogene and the *p53* tumor suppresser gene to allow for analysis of mutant cell behavior in the context of an otherwise normal animal. Cooperation between oncogenic ras and point-mutant *p53* was one of the earliest examples of genetic interaction between two cancer genes (24). Based on the observation that both *K-ras* and *p53* are frequently mutated in human tumors, we expect that the K,P compound mutant mice described in this work will be useful in accurately modeling a number of different types of cancer beyond the advanced pulmonary adenocarcinoma described here.

K,P mice develop advanced lung adenocarcinoma. Through the generation of *K-ras*^{G12D};*p53* compound conditional mice, we have created an improved murine lung adenocarcinoma model that faithfully recapitulates several characteristics of the human disease not commonly observed in previous models. The tumors in these mice exhibit a high degree of nuclear atypia, elicit stromal desmoplasia, and are invasive and metastatic. Although it has been shown in other mouse lung cancer models that *K-ras* and *p53* cooperate in the promotion of tumor growth and progression, the induction of a desmoplastic response and the development of metastatic disease were not reported (4, 5).

Human pulmonary adenocarcinomas often contain a large stromal component. The microenvironment in which a tumor resides may play a critical role in tumor growth and progression, and interactions between cells in the tumor and the microenvironment have been shown to elicit changes in cell behavior (25, 26). The induction of desmoplastic stroma is commonly seen in non–small-cell lung cancer and may contribute to disease progression. The production by stromal fibroblasts of hyaluronan and various matrix metalloproteinases involved in reorganization of the extracellular matrix are thought to influence the invasive and metastatic properties of the tumor (25). Correlative studies suggest that stromal productions of the cell adhesion molecule hyaluronan and of thymidine phosphorylase, which has angiogenic activity, correlate with poor prognosis (27, 28).

Human non–small-cell lung cancer is highly metastatic. Patients diagnosed with early-stage disease that has not spread to lymph nodes or distant organs have an average 5-year survival of about 50%. However, only 15% of lung cancer patients are diagnosed at this stage; most are diagnosed with metastatic disease and have an overall 5-year survival rate only 14%. The current therapeutic regimens are not effective in the treatment of advanced non–small-cell lung cancer. Many murine lung cancer models have been created that provide valuable insights into the molecular alterations driving lung tumorigenesis. However, because these models do not generally develop advanced disease, their growth properties and response to therapeutics may not accurately reflect those of human tumors. Thus, the model described here will provide a valuable system for the study of lung tumor biology and the preclinical testing of novel therapeutics.

The contact mutation p53^{R270H} contributes more strongly to lung tumorigenesis than the structural mutation p53^{R172H}. Although it is generally accepted that p53 mutation is an important event in the development of lung cancer, the relative contribution of different p53 mutations has not been previously analyzed in an *in vivo* setting. By comparing the effects of different *p53* alleles under identical conditions, we have established that loss of p53 function is sufficient to promote the progression of *K-ras* initiated lung adenocarcinomas in mice and that the *p53*^{R270H} allele more

Downloaded from http://aacrjournals.org/cancerres/article-pdf/65/22/10280/2538761/10280-10288.pdf by guest on 27 March 2025

strongly contributes to lung tumorigenesis by acting as a partial dominant-negative. The primary functions of p53 are to respond to cellular stresses by transactivating genes involved in cell cycle arrest, apoptosis, and genome maintenance. Although we could not determine the contribution of specific *p53* effector pathways, it is unlikely that the apoptotic functions of p53 are significant in this setting because we could not detect any differences in the rates of apoptosis within lung tumors of K,P mice by immunostaining for cleaved caspase-3 (data not shown).

Instead, it seems likely that loss of the genome maintenance and antiproliferative functions of p53 are critical to the development of advanced lung adenocarcinoma. One of the most prominent features of the tumors in K;Fl/Fl mice is the development of severe nuclear dysplasia. The observation of lesions with prominent nuclear atypia just 6 weeks after infection with AdenoCre indicates a rapid accumulation of genetic abnormalities following loss of *p53*. Our finding that early-stage K;Fl/Fl, K;270/Fl, and K;172/Fl tumors did not up-regulate the MAPK pathway whereas late-stage tumors did is consistent with this hypothesis. The data show that p53 mutation is not sufficient for up-regulation of this pathway but facilitates the acquisition of additional events leading to increased signaling through the Raf/MAPK pathway.

Loss of p53 seems to affect the progression of lung adenocarcinomas rather than their initiation. Lung tumors are extremely rare in $p53^{-/-}$ mice, presumably due to the early onset of lymphomas and sarcomas. A small subset of $p53^{+/-}$ mice does develop lung adenocarcinomas but the tumors are generally solitary and have a long latency (>18 months). Likewise, $p53^{Fl/Fl}$ mice treated with AdenoCre also develop lung adenocarcinomas but only 1 to 1.5 years after treatment (29). Therefore, p53 mutation alone is not sufficient for the initiation of lung cancer. Instead, activation of *K-ras* serves to initiate the tumor and p53 loss contributes to the progression.

Although p53 loss of function is sufficient to drive tumor progression in *K-ras*-induced lung adenocarcinomas, p53 is rarely deleted in human lung tumors. Rather, p53 is commonly point-mutated at specific hotspot residues in the DNA-binding domain in lung and other tumors. In particular, contact mutations at codons 248 and 273 are very common in human lung adenocarcinomas. In contrast, an analysis of spontaneous tumors from the IARC p53 mutation database (version R9) confirms that codon 175 mutations are substantially underrepresented in adenocarcinomas and non–small-cell lung cancers compared with all tumors (χ^2, $P = 0.000026$). Previously, explanations for this variation focused on the mutagenic effects of cigarette smoke on different p53 codons, especially in light of *in vitro* evidence showing that codon 175 mutations are more potent in oncogenic assays. However, we found that the $p53^{R270H}$ mutation is more strongly dominant-negative over wild-type p53 than is the $p53^{R172H}$ mutation and therefore more effective in tumor promotion as shown by the increased tumor burden and higher proportion of high-grade tumors in K;270/+ mice.

There are many possible explanations for this effect. For example, $p53^{R270H}$ may have a stronger intrinsic capacity to interfere with wild-type p53 than $p53^{R172H}$. Alternatively, $p53^{R270H}$ may accumulate to higher levels in tumor cells than $p53^{R172H}$. Consistently, we found that a higher proportion of K; 270/+ tumors showed strong immunoreactivity for p53 (data not shown). One final possibility is that K;270/+ tumors undergo LOH at an earlier point than K;172/+ tumors, perhaps due to a specific dominant-negative effect by $p53^{R270H}$ on the genome maintenance functions of p53. Once again, our data on tumor grade and MAPK up-regulation are consistent with this hypothesis as discussed above.

Gain-of-function effects of point-mutant p53 in sinonasal adenocarcinoma. In addition to non–small-cell lung cancer, some of the K,P mice developed anaplastic adenocarcinoma of the nasal mucosa arising from the mucous gland epithelium. A significantly

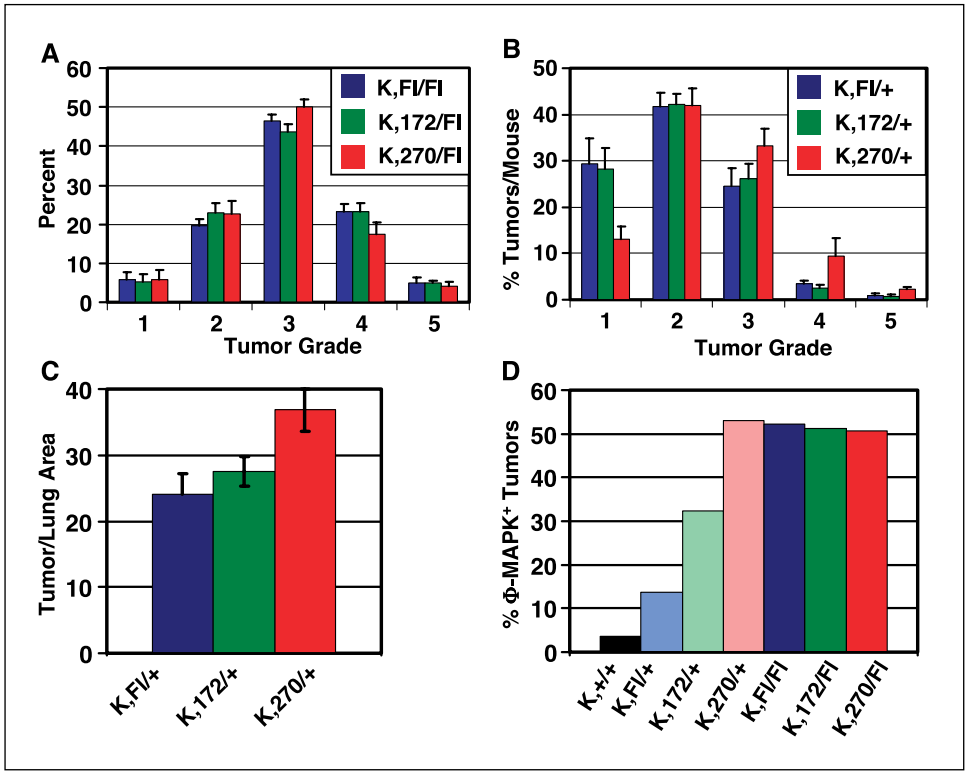

Figure 5. Dominant-negative effects by the contact mutant $p53^{R270H}$. *A,* distribution of tumor grades in K;Fl/Fl mice (*blue columns*), K;172/Fl mice (*green columns*), and K;270/Fl mice (*red columns*). *Columns,* percent of total tumors for each grade; *bars,* SE. *B,* distribution of tumor grades in K;Fl/+ mice (*blue columns*), K;172/+ mice (*green columns*), and K;270/+ mice (*red columns*). *Columns,* percent of total tumors for each grade; *bars,* SE. *C,* areas of tumors in K;Fl/+ mice (*blue columns*), K;172/+ mice (*green columns*), and K;270/+ mice (*red columns*). *Columns,* percent of lung area occupied by tumors; *bars,* SE. *D,* MAPK activation in K,P mice. *Columns,* percent of tumors with positive staining for ϕ-MAPK in the indicated genotypes.

Downloaded from http://aacrjournals.org/cancerres/article-pdf/65/22/10280/2538761/10280-10288.pdf by guest on 27 March 2025

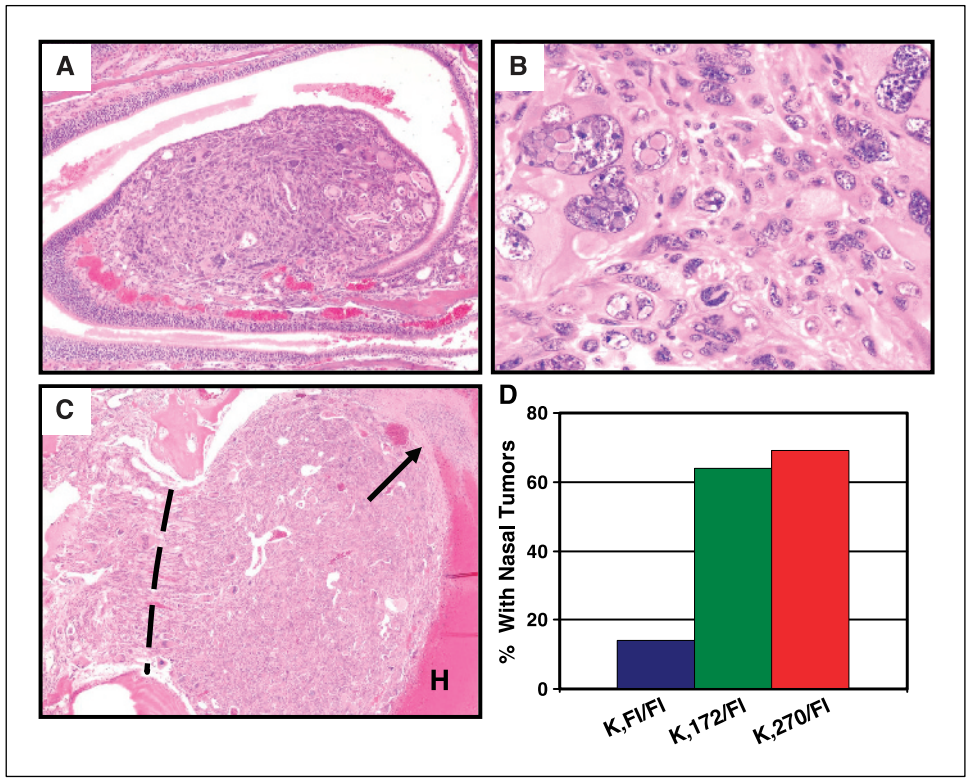

Figure 6. Sinonasal tumors in K,P mutant mice. Slides are stained with H&E. *A,* a small sinonasal adenocarcinoma is shown in the nasal mucosa; ×100. *B,* section of a sinonasal adenocarcinoma from a K;270/Fl mouse. These tumors develop dramatically pleomorphic nuclear atypia; ×400. *C,* section of a sinonasal adenocarcinoma invading the brain. *Dashed line,* location of the cribriform plate. *Arrow,* leading front of the tumor invading into the remains of the olfactory bulb (*H*); ×40. *D,* fractions of K;Fl/Fl, K;172/Fl, and K;270/Fl mice that developed sinonasal adenocarcinoma.

higher proportion of both K;270/Fl and K;172/Fl mice developed sinonasal adenocarcinomas (69% and 64%, respectively) compared with K;Fl/Fl mice (14%). Because the lung tumor phenotype did not vary between K;Fl/Fl and K;270/Fl or K;172/Fl, the discrepancy in sinonasal adenocarcinoma incidence strongly suggests a tissue-specific gain-of-function of point-mutant p53. Also intriguing is the fact that the relative effects of the $p53^{R270H}$ and the $p53^{R172H}$ alleles are similar in the mucous gland epithelium but appreciably different in the lung epithelium, also pointing to the tissue specificity of the effects of individual p53 mutations. Given the prevalence of p53 mutations in human cancer, elucidating the different allele- and tissue-specific effects of mutant p53 is critical to developing a more complete understanding of molecular carcinogenesis.

Sinonasal adenocarcinomas are rare in humans and the tumors seen in our mice are not readily diagnosed based on human classification criteria. However, we believe they arise from the epithelium of the mucous glands and, thus, are most similar to minor salivary gland tumors in humans. The majority of over 500 minor salivary glands in the head and neck are mucous glands (http://www.bcm.edu/oto/grand/7992.html). Minor salivary gland tumors in humans account for only 10% to 15% of all salivary gland tumors but, unlike tumors of the major salivary glands, which are mostly benign, ≥80% of minor salivary gland tumors are malignant (30, 31). Interestingly, although p53 alterations are rare when evaluated in salivary gland carcinomas as a whole, their frequency may be much higher in carcinomas of the minor salivary glands. An analysis of adenoid cystic and mucoepidermoid carcinomas of the salivary glands revealed p53 alterations in 17.6% and 14.8% of the tumors, respectively, but all of these were tumors arising from the minor salivary glands (32). Therefore, p53 mutation may play a critical role in the generation of minor salivary gland tumors.

Surgery is the primary mode of treatment for minor salivary gland tumors, followed by radiation therapy in some cases (31). Unfortunately, due to the rarity, multiplicity of sites of origin, and varied histology of the disease, no large, multi-institutional, prospective, randomized trials have been completed. As such, the current treatment strategies might not be optimal. We believe this model may provide a valuable tool for the study of minor salivary gland carcinoma biology and could aid in the development of better treatment strategies.

Acknowledgments

Received 6/22/2005; revised 9/9/2005; accepted 9/20/2005.

Grant support: Howard Hughes Medical Institute (Physician Postdoctoral Research Fellowship) and American Association for Cancer Research-Pancreatic Cancer Action Network Career Development Award (D.A. Tuveson), David Koch Graduate Fellowship (K.P. Olive), and National Cancer Institute Mouse Models of Human Cancer Consortium.

The costs of publication of this article were defrayed in part by the payment of page charges. This article must therefore be hereby marked *advertisement* in accordance with 18 U.S.C. Section 1734 solely to indicate this fact.

We thank Alice Shaw for helpful discussion and critical reading of the manuscript, Anton Berns for the floxed *p53* mice, and Drs. Werner Rosenau and Harvey Klein for help with histopathology.

References

1. Jemal A, Travis WD, Tarone RE, Travis L, Devesa SS. Lung cancer rates convergence in young men and women in the United States: analysis by birth cohort and histologic type. Int J Cancer 2003;105:101–7.
2. Rodenhuis S, Slebos RJ, Boot AJ, et al. Incidence and possible clinical significance of K-ras oncogene activation in adenocarcinoma of the human lung. Cancer Res 1988;48:5738–41.
3. Meuwissen R, Linn SC, van der Valk M, Mooi WJ, Berns A. Mouse model for lung tumorigenesis through

Downloaded from http://aacrjournals.org/cancerres/article-pdf/65/22/10280/2538761/10280-10288.pdf by guest on 27 March 2025

Cre/lox controlled sporadic activation of the K-Ras oncogene. Oncogene 2001;20:6551–8.
4. Fisher GH, Wellen SL, Klimstra D, et al. Induction and apoptotic regression of lung adenocarcinomas by regulation of a K-Ras transgene in the presence and absence of tumor suppressor genes. Genes Dev 2001;15: 3249–62.
5. Johnson L, Mercer K, Greenbaum D, et al. Somatic activation of the K-ras oncogene causes early onset lung cancer in mice. Nature 2001;410:1111–6.
6. Jackson EL, Willis N, Mercer K, et al. Analysis of lung tumor initiation and progression using conditional expression of oncogenic K-ras. Genes Dev 2001;15: 3243–8.
7. Chiba I, Takahashi T, Nau MM, et al. Mutations in the p53 gene are frequent in primary, resected non-small cell lung cancer. Lung Cancer Study Group. Oncogene 1990;5:1603–10.
8. Olivier M, Eeles R, Hollstein M, Khan MA, Harris CC, Hainaut P. The IARC TP53 database: new online mutation analysis and recommendations to users. Hum Mutat 2002;19:607–14.
9. Smith LE, Denissenko MF, Bennett WP, et al. Targeting of lung cancer mutational hotspots by polycyclic aromatic hydrocarbons. J Natl Cancer Inst 2000;92: 803–11.
10. Cadwell C, Zambetti GP. The effects of wild-type p53 tumor suppressor activity and mutant p53 gain-of-function on cell growth. Gene 2001;277:15–30.
11. Cho Y, Gorina S, Jeffrey PD, Pavletich NP. Crystal structure of a p53 tumor suppressor-DNA complex: understanding tumorigenic mutations [see comments]. Science 1994;265:346–55.
12. Ahrendt SA, Hu Y, Buta M, et al. p53 mutations and survival in stage I non-small-cell lung cancer: results of a prospective study. J Natl Cancer Inst 2003;95:961–70.
13. Mitsudomi T, Hamajima N, Ogawa M, Takahashi T. Prognostic significance of p53 alterations in patients with non-small cell lung cancer: a meta-analysis. Clin Cancer Res 2000;6:4055–63.
14. Sigal A, Rotter V. Oncogenic mutations of the p53 tumor suppressor: the demons of the guardian of the genome. Cancer Res 2000;60:6788–93.
15. Dittmer D, Pati S, Zambetti G, et al. Gain of function mutations in p53. Nat Genet 1993;4:42–6.
16. Olive KP, Tuveson DA, Ruhe ZC, et al. Mutant p53 gain of function in two mouse models of Li-Fraumeni syndrome. Cell 2004;119:847–60.
17. Fasbender A, Lee JH, Walters RW, Moninger TO, Zabner J, Welsh MJ. Incorporation of adenovirus in calcium phosphate precipitates enhances gene transfer to airway epithelia *in vitro* and *in vivo*. J Clin Invest 1998;102:184–93.
18. Tuveson DA, Shaw AT, Willis NA, et al. Endogenous oncogenic K-ras(G12D) stimulates proliferation and widespread neoplastic and developmental defects. Cancer Cell 2004;5:375–87.
19. Jonkers J, Meuwissen R, van der Gulden H, Peterse H, van der Valk M, Berns A. Synergistic tumor suppressor activity of BRCA2 and p53 in a conditional mouse model for breast cancer. Nat Genet 2001;29:418–25.
20. Tuveson DA, Jacks T. Modeling human lung cancer in mice: similarities and shortcomings. Oncogene 1999;18: 5318–24.
21. Lang GA, Iwakuma T, Suh YA, et al. Gain of function of a p53 hotspot mutation in a mouse model of Li-Fraumeni syndrome. Cell 2004;119:861–72.
22. Lin AW, Barradas M, Stone JC, van Aelst L, Serrano M, Lowe SW. Premature senescence involving p53 and p16 is activated in response to constitutive MEK/MAPK mitogenic signaling. Genes Dev 1998;12: 3008–19.
23. Baker SJ, Preisinger AC, Jessup JM, et al. p53 gene mutations occur in combination with 17p allelic deletions as late events in colorectal tumorigenesis. Cancer Res 1990;50:7717–22.
24. Parada LF, Land H, Weinberg RA, Wolf D, Rotter V. Cooperation between gene encoding p53 tumour antigen and ras in cellular transformation. Nature 1984;312:649–51.
25. Liotta LA, Kohn EC. The microenvironment of the tumour-host interface. Nature 2001;411:375–9.
26. Elenbaas B, Weinberg RA. Heterotypic signaling between epithelial tumor cells and fibroblasts in carcinoma formation. Exp Cell Res 2001;264:169–84.
27. Pirinen R, Tammi R, Tammi M, et al. Prognostic value of hyaluronan expression in non-small-cell lung cancer: Increased stromal expression indicates unfavorable outcome in patients with adenocarcinoma. Int J Cancer 2001;95:12–7.
28. Kojima H, Shijubo N, Abe S. Thymidine phosphorylase and vascular endothelial growth factor in patients with stage I lung adenocarcinoma. Cancer 2002;94:1083–93.
29. Meuwissen R, Linn SC, Linnoila RI, Zevenhoven J, Mooi WJ, Berns A. Induction of small cell lung cancer by somatic inactivation of both Trp53 and Rb1 in a conditional mouse model. Cancer Cell 2003;4:181–9.
30. Eveson JW, Cawson RA. Tumours of the minor (oropharyngeal) salivary glands: a demographic study of 336 cases. J Oral Pathol 1985;14:500–9.
31. Strick MJ, Kelly C, Soames JV, McLean NR. Malignant tumours of the minor salivary glands—a 20 year review. Br J Plast Surg 2004;57:624–31.
32. Kiyoshima T, Shima K, Kobayashi I, et al. Expression of p53 tumor suppressor gene in adenoid cystic and mucoepidermoid carcinomas of the salivary glands. Oral Oncol 2001;37:315–22.

Downloaded from http://aacrjournals.org/cancerres/article-pdf/65/22/10280/2538761/10280-10288.pdf by guest on 27 March 2025